Energy 227 (2021) 120518

Contents lists available at ScienceDirect

Energy

journal homepage: www.elsevier.com/locate/energy

# Prediction of performance and exhaust emissions of a CI engine fueled with multi-wall carbon nanotube doped biodiesel-diesel blends using response surface method

Hamit Solmaz [a], Seyed Mohammad Safieddin Ardebili [b], Alper Calam [c, *], Emre Yılmaz [d, e], Duygu İpci [a]

[a] Gazi University, Faculty of Technology, Department of Automotive Engineering, Ankara, Turkey
[b] Department of Biosystems Engineering, Shahid Chamran University of Ahvaz, Ahvaz, Iran
[c] Gazi University, Technical Sciences Vocational High School, Department of Machinery and Metal Technologies, Ankara, Turkey
[d] Sakarya University of Applied Science, Arifiye Vocational High School, Department of Automotive Technology, Sakarya, Turkey
[e] Sakarya University of Applied Sciences Automotive Technologies Application and Research Center, Turkey

ARTICLE INFO

*Article history:*
Received 22 September 2020
Received in revised form
18 March 2021
Accepted 29 March 2021
Available online 2 April 2021

*Keywords:*
Performance
Emissions
Multi-wall carbon nano tubes
Combustion
Biodiesel
Response surface method

ABSTRACT

This study was designed to analyses the performance and exhaust emissions of a direct-injection diesel engine fueled with multi-walled carbon nanotubes (MWCNTs) included in biodiesel-blended diesel fuel using response surface method (RSM). The influence of input parameters —engine load and MWCNTs concentration — on the response parameters (i.e., BSFC, BTE, CO, $NO_X$, and UHC) were investigated and predicted. MWCNTs were added into B20 fuel (20% biodiesel+80% diesel) in various concentrations (25, 50, 75, and 100 ppm). The tests performed under varying engine load conditions (5, 10, 15, and 20 Nm) at a constant engine speed of 1800 rpm. Multi-regression models for BTE, BSFC, and CO, UHC, and $NO_X$ emissions were derived using RSM and were found to be statistically significant. Exhaust UHC and CO concentrations for the studied fuel blend decreases with the addition of MWCNTs into B20 fuel, while NOx emissions drastically increased. The optimal engine working conditions were found to be an engine load of 10 Nm and MWCNTs concentration of 98 ppm. Based on the optimized values, the most optimal results for BTE and BSFC along with CO, UHC, and $NO_X$ emissions were found to be 28.57 (%), 269.84 (g/kWh), 0.03 (%Vol.), 44.16 (ppm), and 458.81 (ppm).



## 1. Introduction

The rapid increase in the world population causes an increase in energy demand as well. The use of fossil-based energy sources in industrial applications causes pollution of clean water sources, and greenhouse gases in the atmosphere increase rapidly [1–5,92,98]. Industrial production has come to a halt due to the COVID-19 pandemic, which has spread around the world recently. Thus, a significant reduction in greenhouse gases in the atmosphere was recorded [6]. Apart from industrial production, internal combustion engines are another cause of greenhouse gases [7].

For this reason, emission values from vehicles are regulated and restricted. Compared to the EURO II emission regulations for passenger cars powered with compression ignition (CI) engines that came into force in 1996 and EURO VI emission standards, which are still in effect today, 4 times improvement in carbon monoxide (CO) and hydrocarbon (HC), 4 times improvement in nitrogen oxide (NOx) and 16 times improvement in soot emissions were requested. It is anticipated that it will be quite challenging to provide the emission regulations in the future with petroleum fuels in SI and CI engines. For this reason, in the near future, spark ignition (SI) and CI engines will be abandoned, and hybrid and electric vehicles will be used [8–17,93–95]. Even if the internal combustion engines are abandoned in passenger cars, the use of CI engines will continue for a while in marine transportation, heavy-duty road vehicles, and public transportation [18,19,97]. For this re, researchers have been working on the usability of alternative fuels in internal combustion engines for a long time. The primary purpose here is to reduce the dependence on fossil oil and to control pollutant exhaust emissions

* Corresponding author.
*E-mail addresses:* hsolmaz@gazi.edu.tr (H. Solmaz), m.safieddin@scu.ac.ir (S.M.S. Ardebili), acalam@gazi.edu.tr (A. Calam), emreylmz@subu.edu.tr (E. Yılmaz), duyguipci@gazi.edu.tr (D. İpci).

https://doi.org/10.1016/j.energy.2021.120518
0360-5442/

with a cleaner combustion by using fuels produced from natural energy sources [20–24]. Alcohols, which have high octane number, can be used as fuel in SI engines and biodiesel produced from vegetable, animal and used waste oils as fuel in CI engines [25–29]. Using vegetable oils and animal fats for biodiesel production may adversely affect food inflation. For this, the use of biodiesel produced from either non-commercial oils or waste oils will reduce fuel costs [30,31].

The oxygen content of biodiesel improves combustion in the cylinder. Thus, HC and CO emissions are reduced. However, the fact that it has a partially lower calorific value compared to pure diesel increases the fuel consumption of biodiesel [32–34]. The main drawbacks of biodiesel is that its lower heating value, high viscosity, and high density compared to diesel [35,36]. High viscosity and density deteriorates atomization during fuel injection. Larger fuel droplet diameter decelerates the mixture preparation. The fuel evaporates more difficult, and the ignition delay period extends. Delaying the combustion process causes CA50 to occur later than the top dead center (TDC). For this reason, thermal efficiency reduces compared to pure diesel [37–39]. There are two ways to overcome this problem. These are increasing injection pressure or using additives to improve the properties of biodiesel fuel [39–42,96].

Addition metallic based nanoparticles to biodiesel and biodiesel-diesel mixture fuels improve flash point, cetane number, and kinematic viscosity properties [43,44]. Metallic additives such as magnesium, manganese, calcium, and copper reduce pollutants such as sulfur dioxide (SO2), carbon dioxide (CO2), and CO [45]. Diesel combustion characteristics improve with the contributions of aluminum oxide ($Al_2O_3$) and copper oxide (CuO) nanoparticles [46]. Another metallic additive that has attracted the attention of researchers in recent years is Multi Walled Carbon Nanotube (MWCNT). MWCNTs are thought to have significant effects on the injection and combustion characteristics of biodiesel fuels. The main reason for these effects is that MWCNTs have a high surface/volume ratio and have the ability to significantly reduce exhaust emissions by acting as catalysts in the combustion zone. Such nano additives improve the heat transfer between the fuel droplets, reduce the ignition delay and improve the ignition temperature of the fuel in the combustion zone [47–49]. Basha and Anand [50] prepared a fuel emulsion by adding 5% water and 2% surfactant to the jatropha biodiesel. Adding water into diesel fuel is one of the preferred methods to reduce exhaust emissions, especially NOx. Besides, in this study, 25, 50, and 100 ppm carbon nanotubes (CNTs) were added into the emulsion fuel. Pure jatropha biodiesel, emulsion fuel, and CNTs doped emulsion fuel results were compared with each other. The results show that the addition of water to the jatropha biodiesel caused micro-explosions, increased performance, and reduced exhaust emissions, especially NOx. With the addition of CNTs to the emulsion fuel, the fuel properties of the biodiesel were improved, and the thermal efficiency increased. Selvan et al. [47] examined the effects of cerium oxide and CNT nano additives on 70% diesel, 10% biodiesel, and 20% ethanol fuel blend. Additionally, nano additives to the blended fuel increased the in-cylinder pressure. Besides, cerium oxide and CNT additives improved fuel properties and enabled combustion to start at earlier crank angles. It was also reported that the nano additives significantly reduced HC emissions by improving combustion. Hosseini et al. [51] conducted a study to investigate the effects of 30, 60, and 90 ppm CNTs addition on B5 and B10 biodiesel-diesel fuel blends on engine performance and exhaust emissions. The highest engine torque and brake thermal efficiency were obtained with 90 ppm CNTs doped B5 fuel. It was found that as the CNTs ratio in mixture fuels increased, CO and HC emissions decreased. However, the increase in gas temperatures after combustion with the contribution of CNTs worsened NOx emissions. Najafi [52] investigated the effect of using pure diesel, pure waste cooking oil biodiesel and biodiesel doped 40, 80, and 120 ppm silver (Ag) and CNTs on the performance, combustion and exhaust emissions. The highest in-cylinder pressure was obtained with CNTs doped biodiesel. However, CNTs addition also increased the pressure rise rate. In the experimental study, it was proved that CNTs additive has a cetane improver effect. Accordingly, the use of CNTs doped biodiesel reduced the ignition delay. With the CNTs additive, CO emissions were considerably reduced compared to pure diesel and pure biodiesel.

By regarding the literature review, it is seen that CNTs additives are used with different rates of biodiesel and in each study. Besides, CNTs addition rates are very variable as well. For this manner, its very complicated to determine the proper CNTs additive amount in the fuel. Response surface methodology is one of the most frequently used methods for optimizing the blends of alternative fuels with petroleum-based fuels in internal combustion engines. RSM techniques could effectively illustrate the relationships between objective functions and multi-factors [53] [–] [58]. Atmanlı et al. [53] were used RSM approach to determined the optimal blend ratios of the diesel, n-butanol and cotton oil ternary blend. They performed experiments at full load and constant engine speed of 2200 rpm. According to the results, the optimum fuel concentrations were found as 65.5% diesel, 23.1% n-butanol and 11.4% cotton oil. İleri et al. [54] investigated the effects of the injection timing and engine speed on engine performance and exhaust emission parameters of a turbocharged diesel engine fueled with canola methyl ester. The experimental design were carried out by using second order full quadratic RSM. It was reported that the optimal values were predicted with an error of 5%. Yilmaz et al. [55] conducted a study to determine the suitability of hazelnut oil methyl ester for a turbocharged direct injection diesel engine. Experiments were carried out at full load and different engine speeds. Engine performance and exhaust emissions were modelled by using RSM and least-square support vector machine (LSSVM) approaches. It was reported that both of them were effective to model the engine performance. It was also reported that the LSSVM method was slightly better than RSM. Ardebili et al. [56] conducted a study on optimization of fusel oil, pure gasoline, and 25%, 50%, and 75% blends by volume. The study was carried out at different engine loads, and the RSM method was used for optimization. Optimization results showed a maximum estimation error of 4% compared to the experimental results. Accordingly, it can be stated that the models obtained by using RSM are satisfactory in terms of engine performance and emissions. In another study, Ardebili et al. [57] performed an multi-objective optimization study using the RSM method for the addition of a nano-biochar additive to the fusel oil-diesel fuel blend. In this study, optimum working conditions are determined for different fusel oil-diesel blend ratios (5%, 10%, 15%, and 20%), different engine speeds (1800, 2000, 2200, 2400 and 2600 rpm) and different rates of nano additive biochar (25, 50, 75, 100 and 125 ppm). The fusel oil ratio, engine speed, and nano additive concentration were selected as input parameters for the analysis. As a result of the analysis, engine torque, engine power, specific fuel consumption (BSFC), and exhaust emissions were examined. RSM results were compared with experimental results. The results showed that the optimum working conditions for the nano-biochar additive were provided by the addition of 100 ppm biochar to the blend of 10% fusel oil and 90% diesel fuel at an engine speed of 2300 rpm. Also, in the RSM analysis, the results were estimated with a value below 5% error. Najafi et al. [58] performed an analysis of experimental results by RSM method in order to determine the optimum engine working conditions of bioethanol-gasoline fuel blends. In the study, performance and exhaust

emissions of 5%, 7.5%, 10%, 12.5%, and 15% bioethanol-gasoline blends were investigated. According to the 98% verified RSM results, optimum working conditions were obtained with a blend of 10% bioethanol-90% gasoline and at an engine speed of 3000 rpm. It was stated that optimum working parameters could be determined with less experimental studies by using the RSM method.

In this study, optimum working conditions of biodiesel-diesel fuel blends doped 25, 50, 75, and 100 ppm MWCNTs were analyzed by the RSM method. The experimental study was carried out on a single-cylinder, water-cooled, and direct injection CI engine at an engine speed of 1800 rpm and at four different loads (5, 10, 15, and 20 Nm). Pure diesel and 20% biodiesel-80% diesel fuel blend (B20) were determined as a base fuel. Biodiesel used in the study was produced from waste cooking oil by transesterification. The input parameters (i.e., engine load and MWCNTs) and their corresponding responses (i.e., BTE, BSFC, CO, UHC, and $NO_X$) for the RSM method have been determined. Additionally, the results of the analysis have been compared with the experimental study.

## 2. Material and methods

In the present study, pure diesel and biodiesel utilized. B20 fuel was obtained by blending 20% biodiesel and 80% diesel by volume. Used cooking oil was used to produce biodiesel via transesterification. Before transesterification, waste cooking oil was filtered and heated up to 120 °C for 1 h to remove the moisture. The transesterification reaction temperature was kept at 60 °C with 20% pure methanol in the presence of 0.5% sodium hydroxide catalyst (NaOH). Fig. 1 shows the stages of the fuel preparation. The biodiesel produced as a result of the transesterification reaction was subjected to purification 5 times and mixed with diesel fuel. A scale with an accuracy of 0.0001 g was used to measure the MWCNT that will doped to B20. It was determined that the fuel properties of the biodiesel met the EN 14214 and ASTM D6751 standards. Solid powder form MWCNTs with a purity of over 96% was used in the study. Dark black colored MWCNTs has a specific surface area of 240 m2/g, and its length is between 15 and 35 μm. Its inner diameter is 2–6 nm and outer diameter is 4–16 nm. 25, 50, 75, and 100 ppm MWCNTs and B20 fuel were blended with an IsoLAB brand ultrasonic homogenizer for 60 min. Table 1 shows some physico-chemical properties of the test fuels.

Performance, combustion and emission characteristics are largely dependent on the physico-chemical properties of the fuel used. The effect of different ratios of MWCNT added to B20 fuel on fuel properties can be seen in Table 1. Addition of MWCNT to B20 fuel significantly improved lower calorific value, flash point, kinematic viscosity and cetane number. However, MWCNT's high thermal conductivity property had a significant effect on engine performance and combustion as well.

Experiments were carried out on a water-cooled, single-cylinder direct injection compression ignition engine. Table 2 provides the technical specifications of the test engine.

A precision scale with a resolution of 0.01 g was used to measure fuel consumption. A DC dynamometer was used to load the engine at certain engine speed. Cussons 98160 brand dynamometer has the capability to absorb 10 kW power at 4000 rpm engine speed. The test bed is illustrated in Fig. 2. In-cylinder pressure was measured with an AVL brand 8QP500c pressure transducer.

The pressure sensor has a sensitivity of 11.96 Pc/bar and a measuring range of 0–150 bar. Pressure signals were amplified by using amplifier on Cussons P4110 combustion analyzer device. Data acquisition was conducted by NI USB6259 card. 1000 pulse encoder was used to collect the in-cylinder pressure with a resolution of 0.36° crank angle. Exhaust emissions were measured by using BoschBEA350 gas analyzer and AVL Dismoke4000. Technical features of the emission devices are given in Table 3. Exhaust emissions measurements were carried out by regarding the test standards of EN ISO 8178–6.

Multi-objective optimization was performed using a desirability-based RSM technique. Historical-data RSM technique was employed to design the key parameters affecting the responses [59]. Design Expert 10.0.0 software was used to predict/optimize statistical models at different engine load (i.e., 5, 10, 15, 25 Nm) and MWCNTs concentrations (i.e., 25, 50, 75, and 100 ppm). Furthermore, Analysis of Variance (ANOVA) was employed to evaluate the significance of the derived models. Fig. 3 presents the RSM flowchart for optimization of engine performance and emissions.

## 3. Results and discussion

### 3.1. Engine performance

#### 3.1.1. Brake thermal efficiency

In this study, ANOVA method was used to assess the statistical significance of the multi-regression models. As found in Table 4, the ANOVA results showed that the generated regression model for brake thermal efficiency (BTE) was significantly fitted to the experimental data at the 5% level. The estimated polynomial


**Fig. 1.** Fuel preparation stages.

**Table 1**
Comparison of physico-chemical properties of experimental fuels.

| | Lover heating value [kJ/kg] | Density [kg/m$^3$ at 15 °C] | Flash point [°C] | Kinematic viscosity [cst at 40 °C] | Cetane number |
|---|---|---|---|---|---|
| Diesel | 44343 | 831.9 | 65 | 2.76 | 55 |
| B20 | 43325 | 843.2 | 76 | 3.19 | 52.5 |
| B20MWCNT25 | 43369 | 843.9 | 74 | 3.15 | 52.9 |
| B20MWCNT50 | 43401 | 845.2 | 71 | 3.09 | 53.4 |
| B20MWCNT75 | 43448 | 846.9 | 69 | 2.97 | 54.1 |
| B20MWCNT100 | 43616 | 848.1 | 67 | 2.95 | 55.3 |

**Table 2**
Technical specifications of the test engine.

| Engine parameters | Specification |
|---|---|
| Brand | Lombardini |
| Number of cylinders | 1 |
| Bore × Stroke, mm$^2$ | 85 × 90 |
| Swept volume, cm$^3$ | 510 |
| Compression ratio | 17.5/1 |
| Power, kW/rpm | 9/3000 |
| Maximum torque, Nm/rpm | 32.8/1800 |
| Nozzle opening pressure, bar | 190 |
| Cooling | Water cooling |

**Table 3**
The specifications of emission devices.

| Analyzer | Bosch BEA350<br>**Operating range** | **Accuracy** |
|---|---|---|
| Lambda | 0.5 to 9.999 | 0.001 |
| NO (ppm) | 0 to 5000 | 1 |
| CO (% vol.) | 0 to 10 | 0.001 |
| $O_2$ (% vol.) | 0 to 22 | 0.01 |
| HC (ppm) | 0 to 9999 | 1 |
| Analyzer | **AVL DiSmoke 4000**<br>**Opacity** | **K-value** |
| Operating range, % | 0–100 | 0.1 |
| Accuracy, m$^{-1}$ | 0–99.99 | 0.01 |

regression model of BTE is given in Eq. (1). The positive and negative signs denote the synergistic and antagonistic effects of each individual term towards the BTE.

$$BTE(\%) = 29.92 + 0.85A + 0.33B - 0.14AB - 0.1A^2 - 1.78\,B^2 - 0.054A^2B + 0.02AB^2 - 0.076A^3 + 0.11B^3 \quad (1)$$

The P-value for both engine load and nanoparticle concentrations was found to be significant at the level of 1% and 5%, respectively. Also, the F-value for MWCNTs was higher than that of engine load, indicating the concentration of nanoparticles in the biodiesel-diesel blends was the most influential parameter on BTE. Besides, statistical indicators for the derived model including coefficient of variation (CV), $R^2$, adjusted $R^2$, and predicted $R^2$ were calculated to be as 0.997, 0.996, 0.85, and 0.993, respectively. As the difference between predicted $R^2$ and adjusted $R^2$ is less than 0.2, therefore, the predicted $R^2$ is in reasonable agreement with the adjusted $R^2$.

The effects of engine load and MWCNTs concentrations on the BTE at engine speed of 1800 rpm are illustrated in Fig. 4 (a) and (b). As can be seen in Fig. 4(a), the BTE increases with the addition of MWCNT into biodiesel-diesel blends due to the combined effect of increased surface/volume ratio and improved combustion process. With increasing nanoparticle concentration from 20 ppm to 100 ppm, the engine BTE improved by ~7.4%. These trends could be attributed to the fact that the inclusion of MWCNTs into biodiesel/diesel fuel could significantly improve the chemical-physical properties of the fuel mixture, such as dynamic viscosity and thermal conductivity [59,60]. Basha et al. [50] found similar trends when CNTs blended into Jatropha biodiesel-diesel fuel. They attributed this finding to the enhanced heat release/combustion rate and micro-explosion phenomenon. Also, Gad and Jayaraj [61], in a very recent experimental work, claimed that the BTE value increased by ~ 6% compared to neat diesel as a result of higher effective fuel surface and lower fuel viscosity. According to 4b, elevating engine load from 10Nm to 16Nm slightly enhanced the BTE by ~8% but dips slightly from 16Nm to 20Nm loads. The

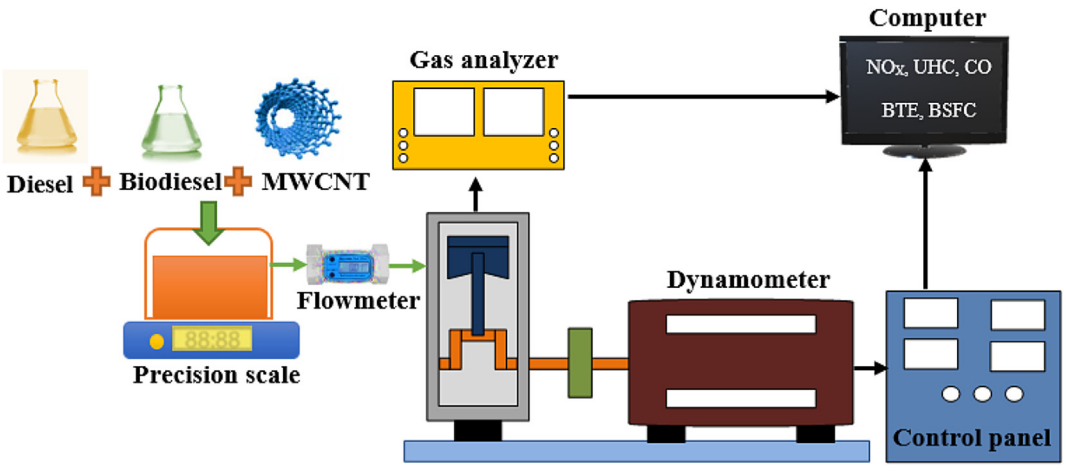


**Fig. 2.** Layout of the test bed.

generation of more brake power at higher engine loads and improvement in combustion efficiency are the main reason for the improvement of BTE [47,62,63]. Besides, an increase in in-cylinder temperature at elevated engine loads could also be considered as another main reason for the increased BTE [64]. The slight decrease in BTE at higher engine loads could be explained by the low excess air-fuel ratio, leading to incomplete combustion [65,66]. At engine load of 20Nm, B20MWCNT100, B20MWCNT75, B20MWCNT50, B20MWCNT25, and pure diesel gave BTE values of 29.03%, 28.54%, 28.09%, 26.86%, and 27.99%, respectively. For all engine loads, the BTE value of the neat diesel is slightly more than the blends of B20MWCNT75, B20MWCNT50, and B20MWCNT25. These comparatively lower BTE could be ascribed to the lower calorific value and energy content of the above-mentioned fuel blends in comparison with neat diesel [67–69].

#### 3.1.2. Brake specific fuel consumption

The fitted multi-regression model based on the coded parameters was predicted using the RSM technique (Eq. (2)). ANOVA method was used to check the significance of the model developed. The F-value indicates the reliability of the mathematical model with the response factor of BSFC.

$$BSFC(\mathrm{g/kWh}) = 258.34 - 3.36A + 6.66B + 1.34AB + 8.33A^2 - 0.44B^2 - 1.09A^2B - 3.32AB^2 + 1.88A^3 - 15.97B^3 \quad (2)$$

The ANOVA results for optimization of brake specific fuel consumption (BSFC) are given in Table 5. As shown in Table 4, the P-value of the model is less than 0.01, indicating the RSM model has high goodness of fit for BSFC. The F-values of 0.52 and 0.88 were obtained for the MWCNTs concentration and engine load, respectively. Considering the F-value, engine load was the most influential parameter affecting the BSFC. The CV of the model (3.96) was found less than 10%, indicating a convincing dependability in the repeated experimental investigations [71]. Besides, the coefficient of determination for the model was 0.98, confirming that 98% of the experimental data give reasonable precision with the output responses. Therefore, the suggested model for BSFC was adequate to explain the relationship between independent and dependent parameters.

Fig. 5 (a) and (b) depict the variation of BSFC of biodiesel-diesel fuel with different dosage levels of MWCNTs additives.

The comparison of results recorded for B20 and pure diesel illustrated that BSFC increased remarkably. The lower heating capacity of the biodiesel in comparison with neat diesel causes slightly elevated BSFC, which is partially compensated by the higher concentration of MWCNTs blended into diesel/biodiesel blends. As can be seen in Fig. 5 (a), MWCNTs incorporation into B20 diminished BSFC values with the minimal BSFC value of 252.12 g/kWh achieved using B20MWCNT100 at an engine load of 20Nm. As depicted in Fig. 5 (b), it could be concluded that the decreasing trend of BSFC could be intensified at higher levels of MWCNTs. As the dosage of MWCNTs in the fuel mixture increased, the BSFC decreased ~8.7%. The decrease in BSFC could be attributed to the positive effect of MWCNTs on the chemical/physical characteristics of fuel mixture, which in turn leading to a reduction in ignition delay time and improvement in the combustion process. As can be seen in Fig. 5 (b), there was also a progressive decrease in BSFC as the engine load increased. Based on the results obtained, with increasing engine load from 10Nm to 20Nm, the BSFC decreased by ~6.7%. At a constant engine speed of 1800 rpm and an engine load of 20Nm, B20MWCNT100, B20MWCNT75, B20MWCNT50, B20MWCNT25, and B20 gave BSFC values of 252.12, 254.77, 256.10, 270.70 and 278.66, respectively. For all engine loads, the BSFC decreases were proportional to the concentration of MWCNTs included in the fuel blends. Such BSFC decrement recorded could be explained by the improved combustion process and decreased amount of heat rejected to coolant water at high levels of engine load [64]. The aforementioned findings are underscored by other studies, showing great potential for the BSFC decrement of MWCNTs/diesel/biodiesel blends [70–74].

### 3.2. Engine emission characteristics

#### 3.2.1. Unburned hydrocarbon emissions

The corresponding RSM-based mathematical model for unburned hydrocarbon (UHC) emissions is shown in Eq. (3).

$$UHC\ emission(\mathrm{ppm}) = 66.75 - 6.54A + 16.91B - 1.78AB + 0.045A^2 - 2.17B^2 - 0.11A^2B - 0.075AB^2 + 0.15A^3 - 0.87B^3 \quad (3)$$

The significance/adequacy of the estimated model were indicated by F- and p-value. The ANOVA results for UHC emission are shown in Table 6. In this study, the F-value for the regression model was 345.4, indicating higher significance of the predicted equation. The p-value for engine load and nanomaterial concentration was also statistically significant at a level of 1%. As shown in Table 6, the effect of engine load on the UHC variation was higher than that of nanomaterial concentration due to its higher F-value (283.97). Considering the model fitting, the obtained $R^2$ was close to 1 (0.9968), showing a highly satisfactory performance ofthe proposed model. Furthermore, the CV of the model was calculated to be 2.8, which is less than 10%.

Fig. 6 (a) and (b) depicts 3D/2D response surface plots for UHC emissions as a function of engine load and MWCNTs concentration. From Fig. 6 (a), the UHC emissions decreased significantly with the inclusion of MWCNTs into the B20 fuel. The improved combustion characteristics and the catalyst activity of MWCNTs could be mentioned as the main reason for such decrement in the UHC emissions quantity. As indicated in Fig. 6(b), a maximum value of UHC emissions was recorded for fuel blend of B20MWCNT25 and engine load of 20Nm, while a minimum amount of UHC emissions was achieved at the engine load of 5Nm and the fuel mixture of B20MWCNT100. The UHC emissions decreased remarkably by ~27%

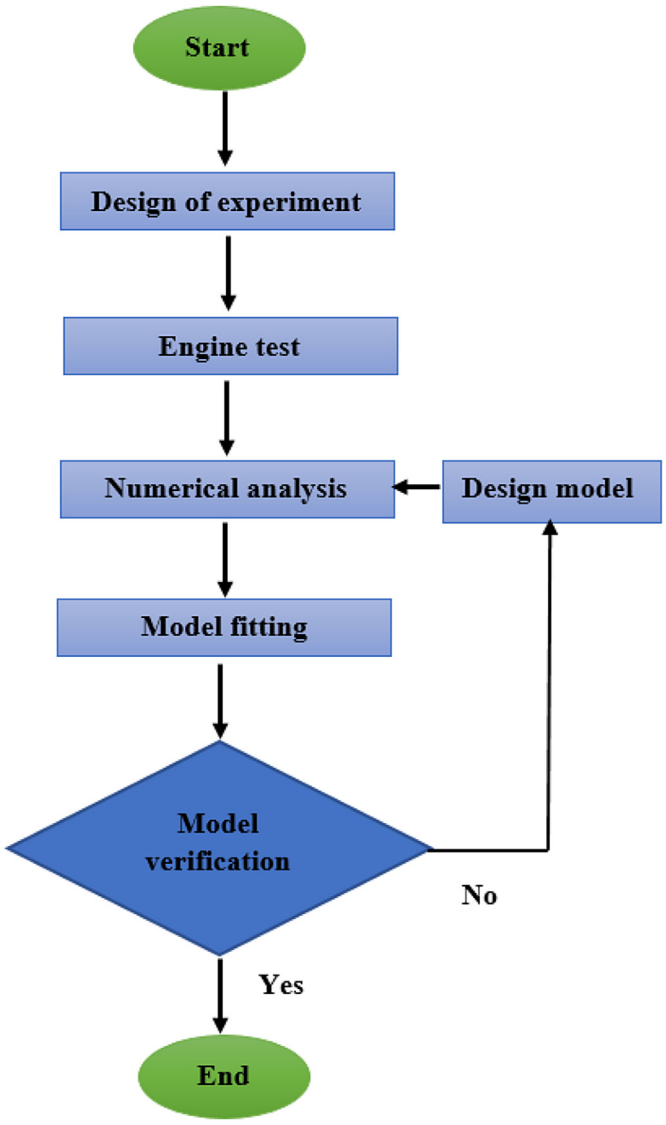


**Fig. 3.** RSM flowchart for optimization of engine performance and emissions.

**Table 4**
ANOVA results for optimization of BTE.

| Source | df | Sum of squares | Mean square | F-value | P-value |
|---|---|---|---|---|---|
| **Model** | 9 | 240.57 | 26.73 | 538.03 | <0.0001 |
| A-MWCNT | 1 | 5.07 | 5.07 | 102.08 | <0.0001 |
| B-Load | 1 | 0.32 | 0.32 | 6.43 | 0.0295 |
| AB | 1 | 0.20 | 0.20 | 4.06 | 0.0717 |
| $A^2$ | 1 | 0.061 | 0.061 | 1.22 | 0.2952 |
| $B^2$ | 1 | 9.71 | 9.71 | 195.52 | <0.0001 |
| $A^2B$ | 1 | 0.20 | 0.20 | 4.11 | 0.0701 |
| $AB^2$ | 1 | 0.017 | 0.017 | 0.34 | 0.5744 |
| $A^3$ | 1 | 0.33 | 0.33 | 6.65 | 0.0275 |
| $B^3$ | 1 | 0.11 | 0.11 | 2.20 | 0.1689 |

when MWCNTs dosage increased up to 100 ppm. However, the UHC emission increased from 49 ppm to 80 ppm in response to increasing engine load from 10Nm to 20Nm, compared to B20 fuel at fixed engine speed condition. For all fuel blends, the UHC emissions was increased at higher engine loads. Such UHC variations could be attributed to the improved vaporization and reduced viscosity of the fuel mixture caused by the addition of nano-additive into diesel/biodiesel mixture [61]. Similar results were also achieved by other researchers, indicating UHC emissions has been reported to decrease when CNTs included in the fuel blend [75–77].

### 3.2.2. Carbon monoxide emissions

The multi-regression model provided by RSM in terms of coded factors is given as the following equation:

$$CO\ emission(\text{ppm}) = 0.038 + 0.002A + 0.009B + 0.0007AB + 0.0001A^2 + 0.011\,B^2 + 0.0039A^2B - 0.0005AB^2 + 0.00041A^3 - 0.0055B^3 \quad (4)$$

The ANOVA results for carbon monoxide (CO) emissions summarized in Table 7. According to the obtained results, nano-additive concentration and engine load had a statistically significant effect (P-value< 0.001) on the formation of CO emissions.

The F-value of 335.53, 22.27, and 120.11 were calculated for the derived model, nano-additive concentration, and engine load, respectively. The P-value of less than 0.01 shows that the developed response surface cubic model adapts every point in the design. Also, the R-square value of 0.9967 and CV value of 3.41 demonstrates the conformity of the employed model. Besides, the adjusted $R^2$, and predicted $R^2$ were calculated to be as 0.993 and 0.982, respectively. The F-value of engine load (120.11) was higher than that of nano-additive (22.27), indicating that the formation of CO emission was most affected by the engine load.

The combined effect of engine load and nano-additive concentration at a constant speed of 1800 rpm on the CO emissions is depicted in Fig. 7 (a) and (b). As can be seen in Fig. 7 (a), the CO emissions was observed to decline with an increase in MWCNTs concentration. According to the results, the CO emissions of B20 fuel was lower compared to pure diesel fuel for all engine loads, mainly due to the higher oxygen content of biodiesel and lower carbon/hydrogen ratio of biodiesel compared to diesel [78,79]. As is shown in Fig. 7 (b), when the concentration of nano-additive increases from 25 ppm to 100 ppm, the CO concentration experiences a dramatic drop by ~43% compared to B20 fuel due to the improved reaction between the fuel and oxygen [80]. The maximum decrease in CO emissions was observed at 100 ppm concentration of the MWCNTs and an engine load of 5Nm. However, increasing engine load from 10Nm to 20Nm results in a significant increase in CO emission levels. The results of the present study have a good agreement with the experimental results from the literature [81–84].

### 3.2.3. Nitrogen oxide emissions

The predicted model for nitrogen oxide ($NO_X$) exhaust emissions was developed from multiple regression analysis techniques. The statistical model based on the coded factors is given in Eq. (5).

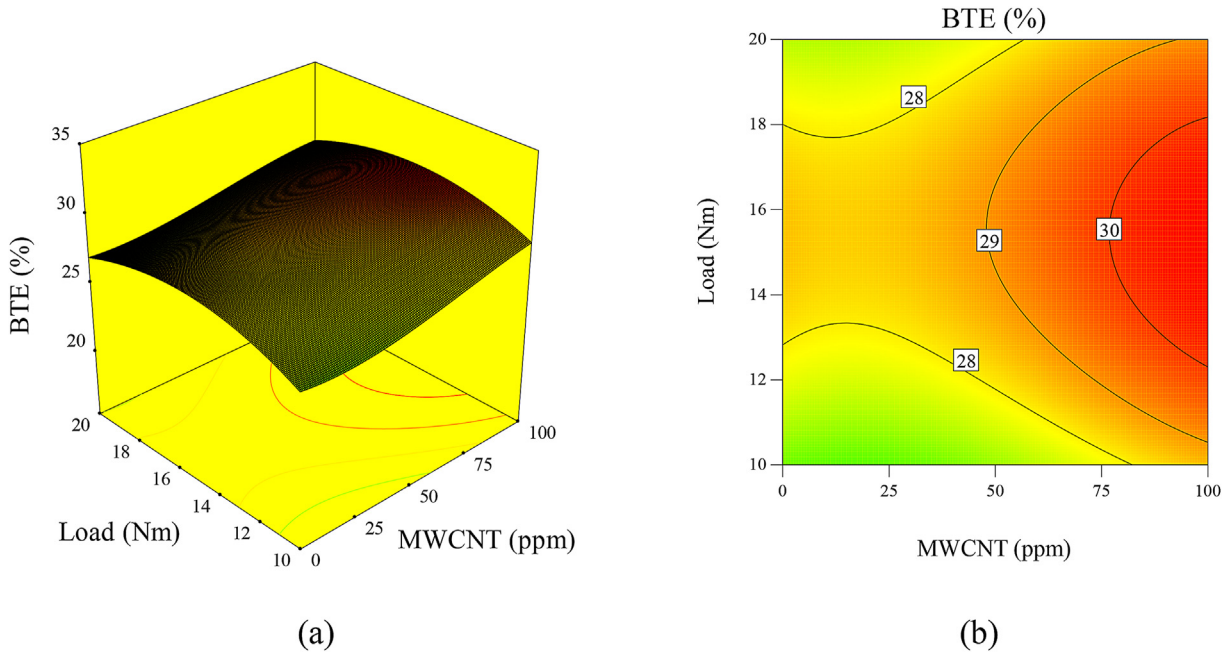


**Fig. 4.** The interactive effect of engine load and nanoparticle concentration on BTE.

**Table 5**
ANOVA results for optimization of BSFC.

| Source | df | Sum of squares | Mean square | F-value | P-value |
|---|---|---|---|---|---|
| Model | 9 | 80895.85 | 8988.43 | 60.10 | <0.0001 |
| A-MWCNT | 1 | 78.52 | 78.52 | 0.52 | 0.4853 |
| B-Load | 1 | 131.50 | 131.50 | 0.88 | 0.3705 |
| AB | 1 | 17.67 | 17.67 | 0.12 | 0.7382 |
| $A^2$ | 1 | 390.67 | 390.67 | 2.61 | 0.1371 |
| $B^2$ | 1 | 0.60 | 0.60 | 4.025E-3 | 0.9507 |
| $A^2B$ | 1 | 83.65 | 83.65 | 0.56 | 0.4718 |
| $AB^2$ | 1 | 440.21 | 440.21 | 2.94 | 0.1170 |
| $A^3$ | 1 | 203.55 | 203.55 | 1.36 | 0.2704 |
| $B^3$ | 1 | 2294.74 | 2294.74 | 15.34 | 0.0029 |

$$NOX\ emission(\text{ppm}) = 545.02 + 40.79A + 130.17B - 1.13AB + 15.27A^2 + 39.83\,B^2 + 2.08A^2B - 3.68AB^2 + 2.7541A^3 + 20.77B^3 \quad (5)$$

Eq. (3) illustrates that MWCNTs concentration (A), engine load (B) have positive effects on the $NO_X$ formation. The Statistical analysis results are shown in Table 8. The model F-value of 417.88 implies that most of the variation in the engine-out $NO_X$ emissions could successfully be estimated by the RSM-based regression model. The F-values of 70.99 and 307.78 were obtained for MWCNTs concentration and engine load, respectively, indicating that these parameters are also significant. The R-square of 0.9973 was calculated for the model, providing a strong correlation between empirical/predicted values. The adjusted $R^2$, predicted $R^2$, and CV of the model were calculated to be as 0.985, 0.9789, and 4.53, respectively. Moreover, the impact of the engine load on the $NO_X$ generation was found to be greater than that of MWCNTs dosage.

The effects of individual factors (i.e., engine load and MWCNTs dosage) on the $NO_X$ emission at engine speed of 1800 rpm are illustrated in Fig. 8 (a) and (b). Overall, could be concluded that the formation of $NO_x$ emissions increases remarkably with increasing engine load as given in Fig. 8 (a). It is well documented that $NO_X$ formation is directly proportional to increased in-cylinder temperature [85]. Based on the experimental results, the $NO_X$ emission for B20 fuel was higher than fossil diesel fuel at all loads. The oxygen content in biodiesel blends is the main reason for increased $NO_X$ concentration [86]. As can be seen in Fig. 8(b), as the dosage of MWCNTs in the fuel blends increases, the $NO_X$ emissions slightly increased for all biodiesel/diesel blends. Also, the amount of engine-out $NO_X$ emissions increased with increase in engine load. As can be seen in Fig. 8 (a), by the addition of 100 ppm MWCNTs into the B20, NOx emission was increased by ~20%. Also, with increasing engine load from 10 Nm to 20 Nm, the concentration of $NO_X$ increased from ~435 ppm to ~735 ppm. However, the least $NO_X$ exhaust emission concentration (219 ppm) was found at an engine load of 5Nm and MWCNTs concentration of 25 ppm. The $NO_X$ emissions for neat diesel, B20, B20MWCNT25 and B20MWCNT50 along with B20MWCNT75, and B20MWCNT100 at engine load of 5Nm were observed to be 212 ppm, 219 ppm, 233 ppm, 266 ppm, 282 ppm, and 318 ppm, respectively. The high in-cylinder peak cycle temperature above 1700 K and longer mixture preparation durations encourage NOx formation in diesel engines. Premixed combustion phase is the main stage for NOx formation because of the more homogeneous mixture prepared during the ignition delay. Its well known that the MWCNT accelerates the atomization and mixture preparation in the cylinder. Its 2000 times greater thermal conductivity compared to diesel enhances evaporation of the fuel [90]. Therefore, as the MWCNT dosage increased in the fuel blend, mixture preparation during the ignition delay is accelerated and as a result, it elevates the $NO_X$ levels of biodiesel/diesel/

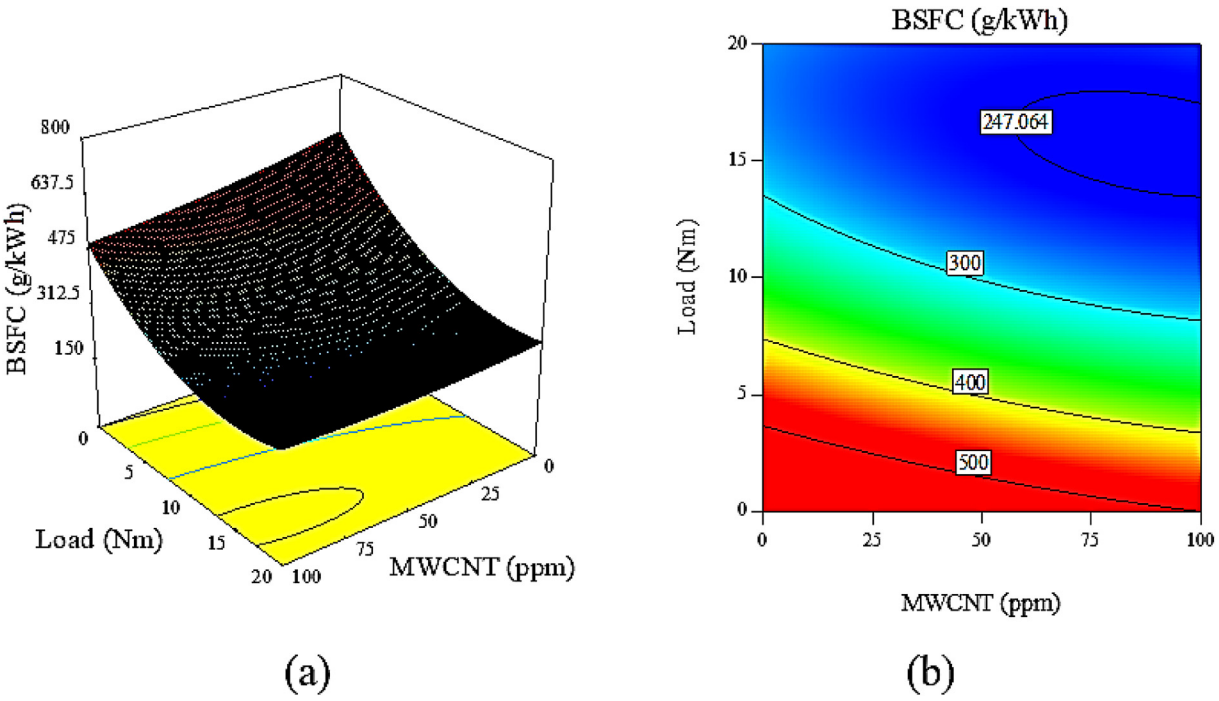


**Fig. 5.** The interactive effect of engine load and nanoparticle concentration on BSFC.

**Table 6**
ANOVA results for optimization of UHC emission.

| Source | df | Sum of squares | Mean square | F-value | P-value |
|---|---|---|---|---|---|
| Model | 9 | 9285.33 | 1031.70 | 345.40 | <0.0001 |
| A-MWCNT | 1 | 297.99 | 297.99 | 99.76 | <0.0001 |
| B-Load | 1 | 848.23 | 848.23 | 283.97 | <0.0001 |
| AB | 1 | 30.99 | 30.99 | 10.38 | 0.0092 |
| $A^2$ | 1 | 0.011 | 0.011 | 3.755E-3 | 0.9523 |
| $B^2$ | 1 | 14.56 | 14.56 | 4.87 | 0.0518 |
| $A^2B$ | 1 | 0.80 | 0.80 | 0.27 | 0.6153 |
| $AB^2$ | 1 | 0.22 | 0.22 | 0.075 | 0.7893 |
| $A^3$ | 1 | 1.22 | 1.22 | 0.41 | 0.5363 |
| $B^3$ | 1 | 6.76 | 6.76 | 2.26 | 0.1634 |

MWCNTs mixture. The findings obtained in this study were in agreement with results of prior works [87–89].

## 4. Response surface optimization

In this study, after developing regression models, a multi-objective optimization technique base on desirability approach was employed to achieve an optimal fuel mixture with the maximum amount of BTE, and minimum value of BSFC and engine-out exhaust emissions (i.e., CO, $NO_X$, and UHC). For each target response, a specific criterion was defined to conduct numerical optimization. The goal, weight, and importance for each input/output term was set as given in Table 9.

The best set of optimal engine working condition and corresponding engine-output responses were identified by comparing all optimal solutions. The results, including the experimental and predicted values for the five responses are listed in Table 10. As can be seen in Table 10, the differences between predicted/experimental data were less than 5%, indicating again that the estimated statistical models in this study are reliable and accurate.

The results indicate that maximum desirability of 0.754 was selected at the engine load of 10Nm and MWCNTs concentration of 98.97 ppm, which could be considered as the optimal engine-operating parameters. Under optimal experimental conditions, the values of BTE and BSFC along with CO, UHC, and $NO_X$ exhaust emissions were found to be 28.57 (%), 269.84 (g/kWh), 0.03 (%Vol.), 44.16 (ppm), and 458.81 (ppm), respectively.

In this study, the optimum engine operating conditions were determined as 1800 rpm engine speed, 10 Nm engine load and 98 ppm MWCNT addition to B20 fuel. Under these conditions, the effects of neat diesel, B20 and B20 + 98 ppm MWCNT-doped fuels on the in-cylinder pressure and heat release rate depending on the crank angle can be seen in Fig. 9. The addition of 20% biodiesel produced from waste frying oil to diesel fuel reduced the in-cylinder peak pressure by 2% compared to pure diesel. However, the peak in-cylinder pressure retarded slightly. The lower calorific value of biodiesel compared to pure diesel reduced the in-cylinder peak pressure when using B20 fuel. In addition, the high viscosity of biodiesel caused the combustion process to be delayed. The addition of MWCNT additive to B20 fuel accelerated the combustion process. MWCNT has a very high thermal conductivity compared to B20 fuel. In addition, MWCNT additive increases the cetane number of diesel-biodiesel blended fuels [72,90,91]. Therefore, the evaporation rate of fuel droplets injected into the cylinder increases, which causes the ignition delay to be reduced. Another factor is the very high surface area/volume ratio of MWCNTs. This increases the heat transfer between particles and fuel droplets [74]. Thus, fuel

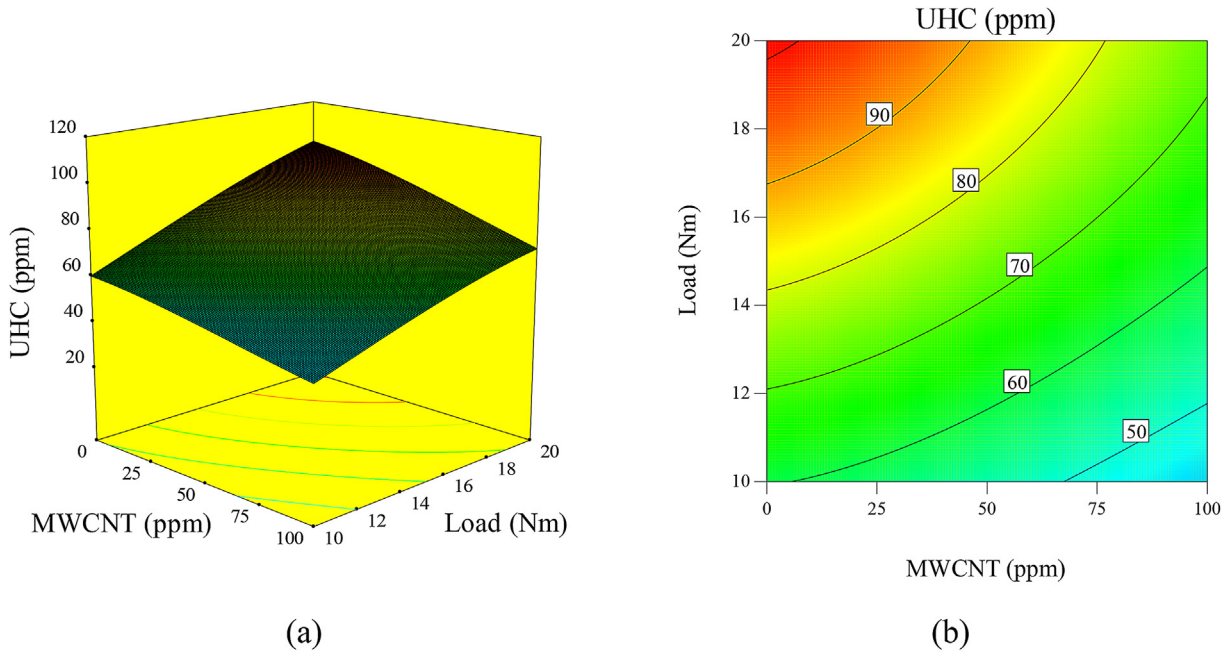


**Fig. 6.** The combined effect of engine load and nano-additive concentration on the UHC emissions.

**Table 7**
ANOVA results for CO exhaust emission.

| Source | df | Sum of squares | Mean square | F-value | P-value |
|---|---|---|---|---|---|
| **Model** | 9 | 6.098E-3 | 6.776E-4 | 335.53 | <0.0001 |
| A-MWCNT | 1 | 4.497E-5 | 4.497E-5 | 22.27 | 0.0008 |
| B-Load | 1 | 2.426E-4 | 2.426E-4 | 120.11 | <0.0001 |
| AB | 1 | 6.154E-8 | 6.154E-8 | 0.030 | 0.8649 |
| $A^2$ | 1 | 1.454E-7 | 1.454E-7 | 0.072 | 0.7939 |
| $B^2$ | 1 | 3.474E-4 | 3.474E-4 | 172.00 | <0.0001 |
| $A^2B$ | 1 | 1.080E-5 | 1.080E-5 | 5.35 | 0.0433 |
| $AB^2$ | 1 | 1.322E-5 | 1.322E-5 | 6.55 | 0.0284 |
| $A^3$ | 1 | 1.0E-7 | 1.000E-7 | 0.050 | 0.8284 |
| $B^3$ | 1 | 2.722E-4 | 2.722E-4 | 134.81 | <0.0001 |

atomization and combustion process improve. These effects can clearly be seen on Fig. 9. The MWCNT doped fuel usage shortened ignition delay and combustion started earlier compared to B20 and neat diesel. This phenomenon proves that injection timing should also be optimized to obtain a further enhancement in BTE and BSFC when the MWCNT doped fuel is used. The highest in-cylinder pressure was achieved as 53.4 bar by adding 98 ppm MWCNT to B20 fuel. At the same operating conditions, the in-cylinder pressure was recorded as 51.49 and 50.63 bar by using pure diesel and B20 fuel, respectively.

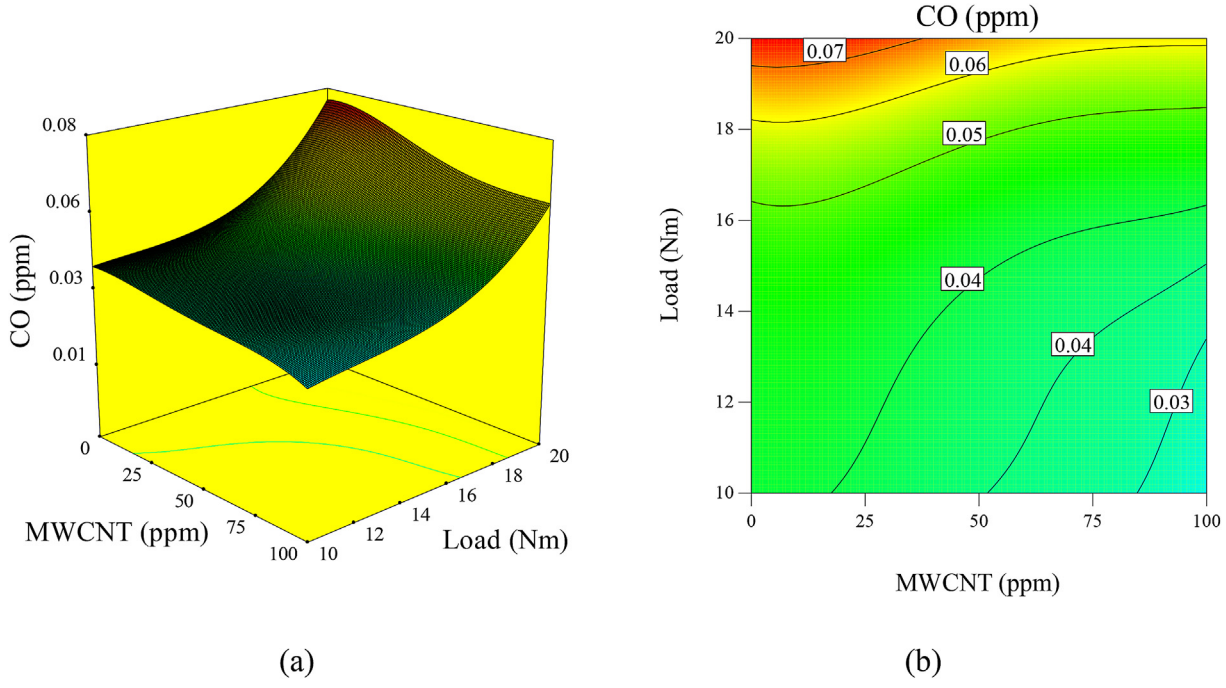


**Fig. 7.** The combined effect of engine load and nano-additive concentration on the CO emission.

**Table 8**
ANOVA results for $NO_X$ exhaust emissions.

| Source | df | Sum of squares | Mean square | F-value | P-value |
|---|---|---|---|---|---|
| **Model** | 9 | 6.143E+5 | 68251.38 | 417.88 | <0.0001 |
| A-MWCNT | 1 | 11594.02 | 11594.02 | 70.99 | <0.0001 |
| B-Load | 1 | 50269.96 | 50269.96 | 307.78 | <0.0001 |
| AB | 1 | 12.45 | 12.45 | 0.076 | 0.7881 |
| $A^2$ | 1 | 1312.58 | 1312.58 | 8.04 | 0.0177 |
| $B^2$ | 1 | 4880.09 | 4880.09 | 29.88 | 0.0003 |
| $A^2B$ | 1 | 302.43 | 302.43 | 1.85 | 0.2035 |
| $AB^2$ | 1 | 540.22 | 540.22 | 3.31 | 0.0990 |
| $A^3$ | 1 | 435.60 | 435.60 | 2.67 | 0.1335 |
| $B^3$ | 1 | 3881.29 | 3881.29 | 23.76 | 0.0006 |

**Table 9**
Numerical optimization criteria for studied parameters.

| Factor | Approach | Limits | | Importance |
|---|---|---|---|---|
| | | Lower | Upper | |
| A: MWCNTs inclusion | In range | 25 | 100 | Medium |
| B: Engine load | In range | 10 | 20 | Medium |
| BTE | Maximize | 19.60 | 30.54 | Medium |
| BSFC | Minimize | 252.12 | 467.09 | Medium |
| CO | Minimize | 0.013 | 0.076 | Medium |
| UHC | Minimize | 29 | 101 | Medium |
| $NO_X$ | Maximize | 219 | 786 | Medium |

## 5. Conclusion

In this work, the RSM has been incorporated using the design expert to optimize diesel engine working parameters fueled with diesel/biodiesel/MWCNTs blends. The influence of different factors— MWCNTs concentration and engine load— on the performance parameters (i.e. BTE and BSFC) and engine-out exhaust emissions (i.e. UHC, $NO_X$, and CO) were examined. Analysis of variance employed to evaluate the significance of the studied parameters and their interactions. Multi-regression model for each response developed and combined effect of input parameters on engine performance/emissions deeply discussed. Increasing engine load from 10Nm to 20Nm significantly enhanced CO, UHC, and $NO_X$ emissions, while increasing MWCNTs from 25 ppm to 100 ppm markedly mitigated aforementioned emissions. Furthermore, the addition of MWCNTs into biodiesel/diesel fuel resulted in a slight increase in BTE. Also, BSFC showed a decreasing trend up to ~8.7% by incorporating MWCNTs into biodiesel/diesel mixture. Desirability function as an efficient technique was successfully applied to

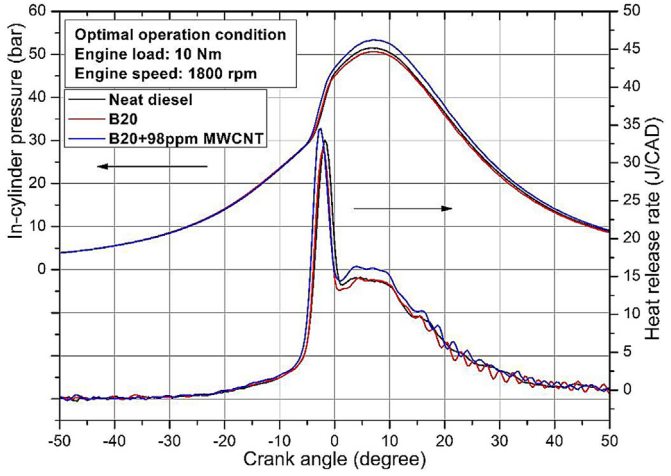


**Fig. 9.** In-cylinder pressure and heat release rate for the optimal operation conditions.

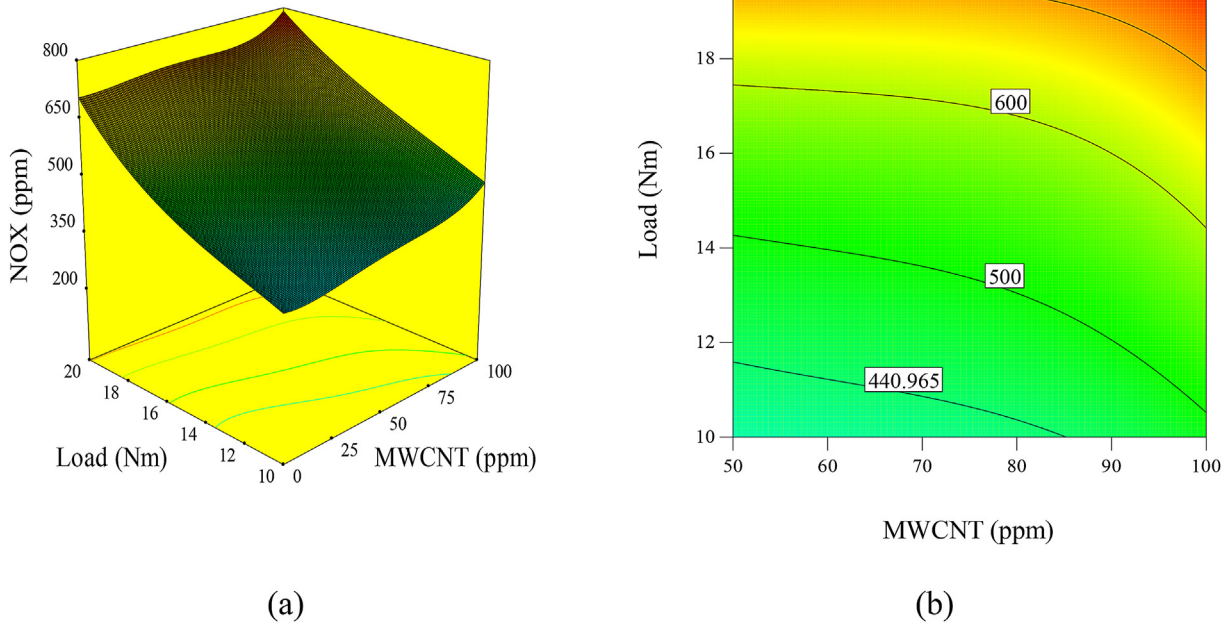


**Fig. 8.** The impacts of engine load and MWCNTs concentration on the emitted $NO_X$ emissions.

**Table 10**
Predicted/experimental data for MWCNT/biodiesel/diesel blends.

| Inputs | | Responses | | | | | | | | | |
|---|---|---|---|---|---|---|---|---|---|---|---|
| | | Experimental | | | | | Predicted | | | | |
| MWCNT (ppm) | Load (Nm) | BTE (%) | BSFC (g/kWh) | CO (%) | UHC (ppm) | $NO_X$ (ppm) | BTE (%) | BSFC (g/kWh) | CO (%) | UHC (ppm) | $NO_X$ (ppm) |
| 25 | 20 | 26.83 | 270.70 | 0.074 | 98 | 710 | 27.10 | 269.75 | 0.074 | 95.99 | 716.03 |
| 25 | 15 | 28.36 | 283.09 | 0.044 | 79 | 501 | 28.41 | 288.91 | 0.044 | 78.84 | 495.54 |
| 25 | 10 | 26.29 | 302.55 | 0.040 | 59 | 385 | 26.08 | 310.78 | 0.039 | 57.64 | 383.08 |
| 25 | 5 | 19.61 | 461.78 | 0.023 | 38 | 233 | 19.46 | 448.69 | 0.024 | 37.59 | 234.34 |
| 50 | 20 | 28.10 | 256.10 | 0.066 | 87 | 729 | 27.77 | 251.21 | 0.067 | 88.80 | 724.44 |
| 50 | 15 | 28.74 | 263.62 | 0.040 | 71 | 516 | 29.04 | 261.92 | 0.040 | 73.19 | 519.15 |
| 50 | 10 | 26.64 | 283.97 | 0.037 | 52 | 409 | 26.72 | 276.54 | 0.037 | 53.37 | 408.51 |
| 50 | 5 | 20.14 | 376.86 | 0.023 | 34 | 266 | 20.14 | 390.89 | 0.022 | 34.56 | 267.91 |
| 75 | 20 | 28.55 | 254.78 | 0.063 | 81 | 731 | 28.59 | 260.62 | 0.062 | 80.61 | 726.51 |
| 75 | 15 | 30.16 | 261.85 | 0.038 | 69 | 525 | 29.92 | 263.22 | 0.038 | 66.75 | 539.90 |
| 75 | 10 | 27.70 | 276.01 | 0.035 | 50 | 438 | 27.71 | 272.78 | 0.035 | 48.53 | 426.92 |
| 75 | 5 | 21.13 | 371.55 | 0.020 | 31 | 282 | 21.28 | 367.58 | 0.020 | 31.16 | 282.66 |
| 100 | 20 | 29.04 | 252.12 | 0.061 | 72 | 786 | 29.08 | 250.43 | 0.061 | 72.30 | 790.14 |
| 100 | 15 | 30.54 | 258.32 | 0.037 | 61 | 627 | 30.60 | 256.69 | 0.036 | 60.40 | 615.61 |
| 100 | 10 | 28.64 | 270.70 | 0.030 | 42 | 477 | 28.60 | 274.78 | 0.030 | 43.99 | 486.03 |
| 100 | 5 | 22.48 | 366.24 | 0.013 | 29 | 318 | 22.43 | 365.48 | 0.013 | 28.29 | 316.21 |
| 0 | 20 | 27.06 | 278.66 | 0.076 | 101 | 707 | 27.02 | 280.36 | 0.076 | 101.30 | 705.88 |
| 0 | 15 | 28.66 | 300.78 | 0.046 | 82 | 485 | 28.48 | 296.92 | 0.045 | 82.83 | 483.79 |
| 0 | 10 | 26.09 | 318.47 | 0.040 | 61 | 371 | 26.25 | 316.82 | 0.041 | 60.46 | 375.45 |
| 0 | 5 | 19.63 | 467.09 | 0.027 | 39 | 219 | 19.70 | 470.89 | 0.027 | 39.40 | 216.87 |

identify optimal input/response parameters in the present study. The optimal engine working conditions were found to be an engine load of 10 Nm and MWCNTs concentration of 98 ppm. At this optimal point, the most optimal results for BTE and BSFC along with CO, UHC, and $NO_X$ emissions were found to be 28.57%, 269.84 g/kWh, 0.03 %Vol., 44.16 ppm, and 458.81 ppm, respectively. Also, the results reveal that the MWCNTs is a promising nano-additive candidate for the reducing CO and UHC emissions of diesel/biodiesel fuel. The outcomes of this study revealed that RSM-based desirability technique can be used as a useful tool to predict diesel engine performance and engine-out emissions.

The present study was conducted within comparatively short operation time and no negative effects of MWCNT additive on engine parts, fuel system or lubricating oil were observed. Also, no carbon deposits were seen on the valve surfaces and valve seats. However, long-term studies about the life of engine components are required to determine such effects. However, the effects of MWCNT in common rail diesel fuel injection systems with high injection pressure can be examined.

## Credit author statement

Hamit Solmaz: Supervision, Conceptualization, Methodology, Writing – original draft, Project administration, Funding acquisition, Validation, Seyed Mohammad Safieddin Ardebili: Methodology, Software, Writing – original draft, Writing – review & editing, Alper Calam: Methodology, Investigation, Writing – review & editing, Emre Yılmaz: Investigation, Writing – review & editing, Duygu İpci: Writing – original draft, Validation, Writing – review & editing,

## Declaration of competing interest

The authors declare that they have no known competing financial interests or personal relationships that could have appeared to influence the work reported in this paper.

## Acknowledgement

This study was supported by Gazi University Projects of Scientific Investigation (BAP) in frame of the project code of 07/2019–14 as researchers, we thank the Gazi University BAP.

## Abbreviations

| | |
|---|---|
| ANOVA | Analysis of variance |
| RSM | Response surface method |
| MWCNT | Multi-walled carbon nanotube |
| BSFC | Brake Specific Fuel Consumption |
| BTE | Brake thermal efficiency |
| LSSVM | Least-square support vector machine |
| B20 | 20% Waste Cooking Oil Biodiesel +80% Diesel |
| B20MWCNT25 | B20 + 25 ppm Multi-walled carbon nanotube |
| B20MWCNT50 | B20 + 50 ppm Multi-walled carbon nanotube |
| B20MWCNT75 | B20 + 75 ppm Multi-walled carbon nanotube |
| B20MWCNT100 | B20 + 100 ppm Multi-walled carbon nanotube |

## References

[1] Barbir F, Veziroğlu TN, Plass Jr HJ. Environmental damage due to fossil fuels use. Int J Hydrogen Energy 1990;15:739–49.
[2] Petrovsky E, Ellwood BB. Magnetic monitoring of air-, land-and water

pollution. Quat Clim Environ Magn 1999:279–322.
[3] Tabanlıgil Calam T. Analytical application of the poly (1H-1, 2, 4-triazole-3-thiol) modified gold electrode for high-sensitive voltammetric determination of catechol in tap and lake water samples. Int J Environ Anal Chem 2019;99:1298–312.
[4] Tabanlıgil CT. Investigation of the electrochemical behavior of phenol using 1H-1, 2, 4-triazole-3-thiol modified gold electrode and its voltammetric determination. J Fac Eng Arch Gazi Univ 2020;35:835–44. https://doi.org/10.17341/gazimmfd.543608.
[5] Calam TT. Electrochemical oxidative determination and electrochemical behavior of 4-nitrophenol based on an Au electrode modified with electropolymerized 3, 5-diamino-1, 2, 4-triazole film. Electroanalysis 2020;1:149–58.
[6] Wang P, Chen K, Zhu S, Wang P, Zhang H. Severe air pollution events not avoided by reduced anthropogenic activities during COVID-19 outbreak. Resour Conserv Recycl 2020;158:104814.
[7] Doucette RT, McCulloch MD. Modeling the prospects of plug-in hybrid electric vehicles to reduce CO2 emissions. Appl Energy 2011;88:2315–23.
[8] Lozhkina OV, Lozhkin VN. Estimation of nitrogen oxides emissions from petrol and diesel passenger cars by means of on-board monitoring: effect of vehicle speed, vehicle technology, engine type on emission rates. Transport Res Transport Environ 2016;47:251–64.
[9] Weiss M, Bonnel P, Kühlwein J, Provenza A, Lambrecht U, Alessandrini S, et al. Will euro 6 reduce the NOx emissions of new diesel cars?–insights from on-road tests with portable emissions measurement systems (PEMS). Atmos Environ 2012;62:657–65.
[10] Zhang Q, Xu Z, Li M, Shao S. Combustion and emissions of a Euro VI heavy-duty natural gas engine using EGR and TWC. J Nat Gas Sci Eng 2016;28:660–71.
[11] Van Mierlo J, Maggetto G, Lataire P. Which energy source for road transport in the future? A comparison of battery, hybrid and fuel cell vehicles. Energy Convers Manag 2006;47:2748–60.
[12] Solmaz H, Kocakulak T. Determination of lithium ion battery characteristics for hybrid vehicle models. Int J Automot Sci Technol 2020;4(4):264–71. https://doi.org/10.30939/ijastech..723043.
[13] Cubito C, Millo F, Boccardo G, Di Pierro G, Ciuffo B, Fontaras G, et al. Impact of different driving cycles and operating conditions on CO2 emissions and energy management strategies of a euro-6 hybrid electric vehicle. Energies 2017;10:1590.
[14] Kocakulak T, Solmaz H. HCCI menzil arttirici motor kullanilan seri hibrit bir aracin modellenmesi. Gazi Üniversitesi Fen Bilimleri Dergisi Part C: Tasarım ve Teknoloji 2020;8(2):279–92. https://doi.org/10.29109/gujsc.670564.
[15] Biçer Y. Thermodynamic analysis of a renewable energy-driven electric vehicle charging station with on-site electricity generation from hydrogen and ammonia fuel cells. Int J Automot Sci Technol 2020;4(4):223–33. https://doi.org/10.30939/ijastech..754580.
[16] emre Ekici Y, Tan N. Charge and discharge characteristics of different types of batteries on a hybrid electric vehicle model and selection of suitable battery type for electric vehicles. Int J Automot Sci Technol n.d.;3:62–70.
[17] Başaran HÜ. Utilizing exhaust valve opening modulation for fast warm-up of exhaust after-treatment systems on highway diesel vehicles. Int J Automot Sci Technol 2020;4:10–22.
[18] Boretti A. The future of the internal combustion engine after “diesel-gate. ” SAE Technical Paper; 2017.
[19] Pierce D, Haynes A, Hughes J, Graves R, Maziasz P, Muralidharan G, et al. High temperature materials for heavy duty diesel engines: historical and future trends. Prog Mater Sci 2019;103:109–79.
[20] Atmanli A, Yilmaz N, et al. An experimental assessment on semi-low temperature combustion using waste oil biodiesel/C3-C5 alcohol blends in a diesel engine. Fuel 2020;260. 116357.
[21] Atmanli A. Experimental comparison of biodiesel production performance of two different microalgae. Fuel 2020;278. 118311.
[22] Yilmaz N, Atmanli A. Sustainable alternative fuels in aviation. Energy 2017;140:1378–86.
[23] Başaran HÜ. A simulation based study to improve active diesel particulate filter regeneration through waste-gate valve opening modulation. Int J Automot Sci Technol 2019;3:32–41.
[24] Yilmaz N, Atmanli A, Trujillo M. Influence of 1-pentanol additive on the performance of a diesel engine fueled with waste oil methyl ester and diesel fuel. Fuel 2017;207:461–9.
[25] Calam A, Solmaz H, Uyumaz A, Yilmaz E, Içingür Y. Investigation of usability of the fusel oil in a single cylinder spark ignition engine, vol. 88; 2015. p. 258–65. https://doi.org/10.1016/j.joei.2014.09.005.
[26] Yilmaz N, İleri E, Atmanli A. Performance of biodiesel/higher alcohols blends in a diesel engine. Int J Energy Res 2016;40(8):1134–43.
[27] Uyumaz A. Combustion, performance and emission characteristics of a DI diesel engine fueled with mustard oil biodiesel fuel blends at different engine loads. Fuel 2018;212:256–67. https://doi.org/10.1016/j.fuel.2017.09.005.
[28] Atmanli A, Ileri E, Yilmaz N. Optimization of diesel–butanol–vegetable oil blend ratios based on engine operating parameters. Energy 2016;96:569–80.
[29] Atmanli A, İleri E, Yüksel B. Effects of higher ratios of n-butanol addition to diesel–vegetable oil blends on performance and exhaust emissions of a diesel engine. J Energy Inst 2015;88(3):209–20.
[30] Demirbas A. Political, economic and environmental impacts of biofuels: a review. Appl Energy 2009;86:S108–17.
[31] Hill J, Nelson E, Tilman D, Polasky S, Tiffany D. Environmental, economic, and energetic costs and benefits of biodiesel and ethanol biofuels. Proc Natl Acad Sci Unit States Am 2006;103:11206–10.
[32] Fang Q, Fang J, Zhuang J, Huang Z. Effects of ethanol–diesel–biodiesel blends on combustion and emissions in premixed low temperature combustion. Appl Therm Eng 2013;54:541–8.
[33] Ng HK, Gan S. Combustion performance and exhaust emissions from the non-pressurised combustion of palm oil biodiesel blends. Appl Therm Eng 2010;30:2476–84.
[34] Ö Can, Öztürk E, Solmaz H, Aksoy F, Çinar C, Yücesu HS. Combined effects of soybean biodiesel fuel addition and EGR application on the combustion and exhaust emissions in a diesel engine. Appl Therm Eng 2016;95:115–24. https://doi.org/10.1016/j.applthermaleng.2015.11.056.
[35] Tashtoush G, Al-Widyan MI, Al-Shyoukh AO. Combustion performance and emissions of ethyl ester of a waste vegetable oil in a water-cooled furnace. Appl Therm Eng 2003;23:285–93.
[36] Nabi MN, Rahman MM, Akhter MS. Biodiesel from cotton seed oil and its effect on engine performance and exhaust emissions. Appl Therm Eng 2009;29:2265–70.
[37] Ganapathy T, Gakkhar RP, Murugesan K. Influence of injection timing on performance, combustion and emission characteristics of Jatropha biodiesel engine. Appl Energy 2011;88:4376–86.
[38] Uyumaz A. Experimental evaluation of linseed oil biodiesel/diesel fuel blends on combustion, performance and emission characteristics in a DI diesel engine. Fuel 2020;267:117150. https://doi.org/10.1016/j.fuel.2020.117150.
[39] Qi D, Leick M, Liu Y, Chia-fon FL. Effect of EGR and injection timing on combustion and emission characteristics of split injection strategy DI-diesel engine fueled with biodiesel. Fuel 2011;90:1884–91.
[40] Kannan GR, Karvembu R, Anand R. Effect of metal based additive on performance emission and combustion characteristics of diesel engine fuelled with biodiesel. Appl Energy 2011;88:3694–703.
[41] Soudagar MEM, Nik-Ghazali N-N, Kalam MA, Badruddin IA, Banapurmath NR, Khan TMY, et al. The effects of graphene oxide nanoparticle additive stably dispersed in dairy scum oil biodiesel-diesel fuel blend on CI engine: performance, emission and combustion characteristics. Fuel 2019;257:116015.
[42] Park SH, Yoon SH, Lee CS. Effects of multiple-injection strategies on overall spray behavior, combustion, and emissions reduction characteristics of biodiesel fuel. Appl Energy 2011;88:88–98.
[43] Heydari-Maleney K, Taghizadeh-Alisaraei A, Ghobadian B, Abbaszadeh-Mayvan A. Analyzing and evaluation of carbon nanotubes additives to diesohol-B2 fuels on performance and emission of diesel engines. Fuel 2017;196:110–23. https://doi.org/10.1016/j.fuel.2017.01.091.
[44] Shaafi T, Sairam K, Gopinath A, Kumaresan G, Velraj R, Shaa T, et al. Effect of dispersion of various nanoadditives on the performance and emission characteristics of a CI engine fuelled with diesel, biodiesel and blends—a review. Renew Sustain Energy Rev 2015;49:563–73. https://doi.org/10.1016/j.rser.2015.04.086.
[45] Gürü M, Karakaya U, Altıparmak D, Alıcılar A. Improvement of diesel fuel properties by using additives. Energy Convers Manag 2002;43:1021–5.
[46] Gumus S, Ozcan H, Ozbey M, Topaloglu B. Aluminum oxide and copper oxide nanodiesel fuel properties and usage in a compression ignition engine. Fuel 2016;163:80–7.
[47] Selvan VAM, Anand RB, Udayakumar M. Effect of Cerium Oxide Nanoparticles and Carbon Nanotubes as fuel-borne additives in Diesterol blends on the performance, combustion and emission characteristics of a variable compression ratio engine. Fuel 2014;130:160–7. https://doi.org/10.1016/j.fuel.2014.04.034.
[48] Tewari P, Doijode E, Banapurmath NR, Yaliwal VS. Experimental investigations on a diesel engine fuelled with multiwalled carbon nanotubes blended biodiesel fuels. Int J Emerg Technol Adv Eng 2013;3:72–6.
[49] El-Seesy AI, Abdel-Rahman AK, Bady M, Ookawara S. Performance, combustion, and emission characteristics of a diesel engine fueled by biodiesel-diesel mixtures with multi-walled carbon nanotubes additives. Energy Convers Manag 2017;135:373–93.
[50] Basha JS, Anand RB. Performance, emission and combustion characteristics of a diesel engine using Carbon Nanotubes blended Jatropha Methyl Ester Emulsions. Alexandria Eng J 2014;53:259–73. https://doi.org/10.1016/j.aej.2014.04.001.
[51] Hassan S, Taghizadeh-alisaraei A, Ghobadian B, Abbaszadeh-mayvan A. Performance and emission characteristics of a CI engine fuelled with carbon nanotubes and diesel-biodiesel blends. Renew Energy 2017;111:201–13. https://doi.org/10.1016/j.renene.2017.04.013.
[52] Najafi G. Diesel engine combustion characteristics using nano-particles in biodiesel- diesel blends 2018;212:668–78. https://doi.org/10.1016/j.fuel.2017.10.001.
[53] Atmanlı A, Yüksel B, İleri E, Karaoglan AD. Response surface methodology based optimization of diesel–n-butanol–cotton oil ternary blend ratios to improve engine performance and exhaust emission characteristics. Energy Conv Manag 2015;90:383–94.
[54] İleri E, Karaoglan AD, Atmanli A. Response surface methodology based prediction of engine performance and exhaust emissions of a diesel engine fuelled with canola oil methyl ester. J Renew Sustain Energy 2013;5(3):033132.
[55] Yilmaz N, İleri E, Atmanlı A, Deniz Karaoglan A, Okkan U, Sureyya Kocak M. Optimization of operating factors and blended levels of diesel, biodiesel and

ethanol fuels to minimize exhaust emissions of diesel engine using response surface methodology. J Energy Resour Technol 2016;138(5):052206.
[56] Safieddin Ardebili SM, Solmaz H, Mostafaei M. Optimization of fusel oil – gasoline blend ratio to enhance the performance and reduce. emissions 2019;148:1334–45. https://doi.org/10.1016/j.applthermaleng.2018.12.005.
[57] Safieddin Ardebili SM, Taghipoor A, Solmaz H, Mostafaei M, Method RS, Safieddin Ardebili SM, et al. The effect of nano-biochar on the performance and emissions of a diesel engine fueled with fusel oil-diesel fuel. Fuel 2020;268:117356. https://doi.org/10.1016/j.fuel.2020.117356.
[58] Najafi G, Ghobadian B, Yusaf T, Safieddin Ardebili SM, Mamat R. Optimization of performance and exhaust emission parameters of a SI (spark ignition) engine with gasoline–ethanol blended fuels using response surface methodology. Energy 2015;90:1815–29. https://doi.org/10.1016/j.energy.2015.07.004.
[59] Sharifi S, Rahimi R, Mohebbi-Kalhori D, Colpan CO. Coupled computational fluid dynamics-response surface methodology to optimize direct methanol fuel cell performance for greener energy generation. Energy 2020;198:117293.
[60] Fayyazbakhsh A, Pirouzfar V. Comprehensive overview on diesel additives to reduce emissions, enhance fuel properties and improve engine performance. Renew Sustain Energy Rev 2017;74:891–901. https://doi.org/10.1016/j.rser.2017.03.046.
[61] Soudagar MEM, Kalam A, Badruddin IA, Banapurmath NR, Akram N. The effect of nano-additives in diesel-biodiesel fuel blends : a comprehensive review on stability , engine performance and emission characteristics the effect of nano-additives in diesel-biodiesel fuel blends : a comprehensive review on stability , engine performance and emission characteristics. Energy Convers Manag 2018;178:146–77. https://doi.org/10.1016/j.enconman.2018.10.019.
[62] Gad MS, Jayaraj S. A comparative study on the effect of nano-additives on the performance and emissions of a diesel engine run on Jatropha biodiesel. Fuel 2020;267:117168.
[63] Rosha P, Mohapatra SK, Mahla SK, Cho H, Chauhan BS, Dhir A. Effect of compression ratio on combustion, performance, and emission characteristics of compression ignition engine fueled with palm (B20) biodiesel blend. Energy 2019;178:676–84.
[64] Suresh M, Jawahar CP, Richard A. A review on biodiesel production, combustion, performance, and emission characteristics of non-edible oils in variable compression ratio diesel engine using biodiesel and its blends. Renew Sustain Energy Rev 2018;92:38–49.
[65] Ashok B, Nanthagopal K, Saravanan B, Azad K, Patel D, Sudarshan B, et al. Study on isobutanol and Calophyllum inophyllum biodiesel as a partial replacement in CI engine applications. Fuel 2019;235:984–94.
[66] Wei L, Cheung CS, Huang Z. Effect of n-pentanol addition on the combustion, performance and emission characteristics of a direct-injection diesel engine. Energy 2014;70:172–80.
[67] Li L, Wang J, Wang Z, Liu H. Combustion and emissions of compression ignition in a direct injection diesel engine fueled with pentanol. Energy 2015;80:575–81.
[68] Tayari S, Abedi R, Rahi A. Comparative assessment of engine performance and emissions fueled with three different biodiesel generations. Renew Energy 2020;147:1058–69.
[69] Vellaiyan S. Combustion, performance and emission evaluation of a diesel engine fueled with soybean biodiesel and its water blends. Energy 2020:117633.
[70] Simsek S. Effects of biodiesel obtained from Canola, sefflower oils and waste oils on the engine performance and exhaust emissions. Fuel 2020;265:117026.
[71] Şahin S, Pekel AG, Toprakçı İ. Sonication-assisted extraction of Hibiscus sabdariffa for the polyphenols recovery: application of a specially designed deep eutectic solvent. Biomass Convers Biorefinery 2020:1–11.
[72] Senthilkumar R, Prabu M. Performance and emission characteristics of single cylinder ci diesel engine using multiwalled nanotubes and karanja oil methyl ester. J Chem Pharmaceut Sci 2015;6:109–14.
[73] Elwardany AE, Marei MN, Eldrainy Y, Ali RM, Ismail M, El-Kassaby MM. Improving performance and emissions characteristics of compression ignition engine: effect of ferrocene nanoparticles to diesel-biodiesel blend. Fuel 2020;270:117574.
[74] Mirzajanzadeh M, Tabatabaei M, Ardjmand M, Rashidi A, Ghobadian B, Barkhi M, et al. A novel soluble nano-catalysts in diesel–biodiesel fuel blends to improve diesel engines performance and reduce exhaust emissions. Fuel 2015;139:374–82.
[75] El-Seesy AI, Hassan H. Investigation of the effect of adding graphene oxide, graphene nanoplatelet, and multiwalled carbon nanotube additives with n-butanol-Jatropha methyl ester on a diesel engine performance. Renew Energy 2019;132:558–74.
[76] El-Seesy A I, Hassan H, Ookawara S. Influence of adding multiwalled carbon nanotubes to waste cooking oil biodiesel on the performance and emission characteristics of a diesel engine: an experimental investigation. Int J Green Energy 2019;16:901–16.
[77] Singh N, Bharj RS. Experimental investigation on the role of indigenous carbon nanotube emulsified fuel in a four-stroke diesel engine. Proc Inst Mech Eng Part C J Mech Eng Sci 2016;230:2046–59. https://doi.org/10.1177/0954406215586021.
[78] Vellaiyan S. Enhancement in combustion, performance, and emission characteristics of a diesel engine fueled with diesel, biodiesel, and its blends by using nanoadditive. Environ Sci Pollut Res 2019;26:9561–73.
[79] Sakthivadivel D, Ganesh Kumar P, Stephen S, Vigneswaran VS, Iniyan S. Experimental investigation of doped mwcnts on biodiesel for enhancement of the performance and exhaust emissions in a diesel engine. Fullerenes, Nanotub Carbon Nanostruct 2019;27:358–66.
[80] Xue J, Grift TE, Hansen AC. Effect of biodiesel on engine performances and emissions. Renew Sustain Energy Rev 2011;15:1098–116.
[81] Bournay L, Casanave D, Delfort B, Hillion G, Chodorge JA. New heterogeneous process for biodiesel production: a way to improve the quality and the value of the crude glycerin produced by biodiesel plants. Catal Today 2005;106:190–2.
[82] Szybist JP, Song J, Alam M, Boehman AL. Biodiesel combustion, emissions and emission control. Fuel Process Technol 2007;88:679–91.
[83] Gürü M, Koca A. Can Ö, Çınar C, Şahin F. Biodiesel production from waste chicken fat based sources and evaluation with Mg based additive in a diesel engine. Renew Energy 2010;35:637–43.
[84] Keskin A, Gürü M, Altıparmak D. Biodiesel production from tall oil with synthesized Mn and Ni based additives: effects of the additives on fuel consumption and emissions. Fuel 2007;86:1139–43.
[85] Janakiraman S, Lakshmanan T, Chandran V, Subramani L. Comparative behavior of various nano additives in a DIESEL engine powered by novel Garcinia gummi-gutta biodiesel. J Clean Prod 2020;245:118940.
[86] Venu H, Subramani L, Raju VD. Emission reduction in a DI diesel engine using exhaust gas recirculation (EGR) of palm biodiesel blended with TiO2 nano additives. Renew Energy 2019;140:245–63.
[87] Köse S, Aylanşık G, Babagiray M, Kocakulak T. Biodiesel production from waste sunflower oil and engine performance tests. Int J Automot Sci Technol 2020;4(4):206–12. https://doi.org/10.30939/ijastech..770309.
[88] Ganesan N, Masimalai S. Experimental investigation on a performance and emission characteristics of single cylinder diesel engine powered by waste orange peel oil biodiesel blended with antioxidant additive. Energy Sources, Part A Recover Util Environ Eff 2020;42:1412–23.
[89] Dhahad HA, Chaichan MT. The impact of adding nano-Al2O3 and nano-ZnO to Iraqi diesel fuel in terms of compression ignition engines' performance and emitted pollutants. Therm Sci Eng Prog 2020:100535.
[90] Gharehghani A, Pourrahmani H. Performance evaluation of diesel engines (PEDE) for a diesel-biodiesel fueled CI engine using nano-particles additive. Energy Convers Manag 2019;198:111921. https://doi.org/10.1016/j.enconman.2019.111921.
[91] Kumar ARM, Kannan M, Nataraj G. A study on performance, emission and combustion characteristics of diesel engine powered by nano-emulsion of waste orange peel oil biodiesel. Renew Energy 2020;146:1781–95. https://doi.org/10.1016/j.renene.2019.06.168.
[92] Tabanlıgil Calam T. Electrochemical behavior and voltammetric determination of 2-nitrophenol on glassy carbon electrode surface modified with 1-amino-2-naphthol-4-sulphonic acid. Eng Perspect 2021;1(1):1–5. https://doi.org/10.29228/sciperspective.48525.
[93] Aydogan B. Combustion, performance and emissions of ethanol/n heptane blends in HCCI engine. Eng Perspect 2021;1(1):6–10. https://doi.org/10.29228/sciperspective.47890.
[94] Yurdaer E, Kocakulak T. Comparison of energy consumption of different electric vehicle power systems using fuzzy logic-based regenerative braking. Eng Perspect 2021;1(1):11–21. https://doi.org/10.29228/sciperspective.47590.
[95] Karaman M, Öztürk E. Analysis of the behavior of a cross-type hydraulic outrigger and stabilizer operating under determined loads. Eng Perspect 2021;1(1):22–9. https://doi.org/10.29228/sciperspective.49248.
[96] Köse S, Babagiray M, Kocakulak T. Response surface method based optimization of the viscosity of waste cooking oil biodiesel. Eng Perspect 2021;1(1):30–7. https://doi.org/10.29228/sciperspective.49697.
[97] Solmaz H., İpci D. Control Of Combustion Phase with Direct Injection Timing for Different Inlet Temperatures in an RCCI Engine. Isı Bilimi ve Tekniği Dergisi 40;2:267–279. doi:10.47480/isibted.817027.
[98] Tabanlıgil Calam T, Yılmaz EB. Electrochemical determination of 8-hydroxyquinoline in a cosmetic product on a glassy carbon electrode modified with 1-amino-2-naphthol-4-sulphonic acid. Instrument Sci Technol 2021;49(1):1–20. https://doi.org/10.1080/10739149.2020.1765175.